Consistent Variational Nodal Diffusion Method Embedded in Method of Characteristics

Kyung Min Kim, Han Gyu Lee, Hyung Jin Shim*
Seoul National University, 1 Gwanak-ro, Gwanak-gu, Seoul 08826
**Corresponding author: shimhj@snu.ac.kr*

1. Introduction

As the nuclear industries shifted their interests to advanced reactors, many institutes have focused on developing neutronics codes capable of unstructured mesh treatment. Griffin [1] and PROTEUS-MOC [2] are representative deterministic codes that successfully incorporate finite element mesh. NuDEAL [3] has been recently developed, confirming that GPU employment is still effective in the planar method of characteristics (MOC) operating over the unstructured mesh geometry.

Several methodologies have been sought to extend the solution capability of NuDEAL from 2D to 3D. The traditional 2D/1D approaches are excluded due to the stability and accuracy issues. The discontinuous Galerkin method-based MOC [2] was implemented and tested in NuDEAL. However, it was shown that the methodology is inefficient when accelerated with GPUs [4].

Meanwhile, the variational nodal method (VNM) [5], based on the hybrid finite element method (FEM) [6], has been employed in various neutronics codes for decades, such as VARIANT [7] and ERANOS [8]. This method was devised as transport solvers involving discrete ordinate (S_N) or spherical harmonics (P_N) methods. Therefore, VNM can be naturally reduced to the diffusion (P_1) formulation. In addition to this, the polynomial order can be arbitrarily modified to improve the solution's accuracy.

In this regard, VNM is being investigated to employ as a low-order 3D solver coupled with planar MOC over the unstructured mesh geometry. Before extending to 3D solution capability, the equivalence between VNM and MOC in 2D problems should be established. This paper deals with the equivalence factors configured under the MOC/VNM scheme. Then, verifications are given for several problems ranging from an assembly problem to a 2D core problem. Furthermore, the effectiveness of the low-order VNM is compared with coarse mesh finite difference (CMFD), a standard acceleration method for transport calculation.

2. Background and Methodologies

2.1. Variational Nodal Diffusion Formulation

The VNM formulation is briefly given here, which is explained in several papers in detail [5][9]. Also, the application is restricted to diffusion formulation. The variational weak form can be written as the following block matrix equation after the Ritz procedure is applied by using the orthogonal bases:

$$\begin{bmatrix} \mathbf{A} & \mathbf{M} \\ \mathbf{M}^T & 0 \end{bmatrix} \begin{bmatrix} \phi \\ J \end{bmatrix} = \begin{bmatrix} s \\ 0 \end{bmatrix}, \tag{1}$$

where ϕ is the even-parity flux moment defined within a volume, J is the odd-parity flux moment on a surface, and s is the volumetric source moment. Here, volumetric variables are expanded by an orthogonal basis set normalized to each element's volume, while an orthonormal one is used for the surface variables. In the diffusion formulation, even- and odd-parity fluxes are equivalent to the scalar flux and the neutron current, respectively. The upper part of Eq. (1) represents the moment-based nodal balance equation described as follows:

$$\mathbf{A}_K \phi_K + \sum_{E \in K} \mathbf{M}_E J_E = s_K, \tag{2}$$

where K is the element index, and E is the face index of the element. The group index is omitted for brevity. Matrix $\mathbf{A}$ involves the diffusion coefficient and the removal cross section (XS) multiplied by the stiffness and mass matrix, respectively. Matrix $\mathbf{M}$ is defined on each face E of element K, which converts the surface variables to the volumetric ones. Multiplied by the surface current J, the term represents the leakage distribution through surface E. The rank of this system is determined by the polynomial order for approximating the volumetric flux distribution.

The lower part of Eq. (1) is the weak continuity imposed on the surface flux moment. This can be expressed for each surface as:

$$\mathbf{M}_{E+}^T \phi_+ = \mathbf{M}_{E-}^T \phi_- \tag{3}$$

where plus and minus signs indicate the downwind and upwind elements which share the surface E, respectively. The polynomial order for the surface current determines this system's rank, which is independent of the volumetric polynomial order. Ranks of Eq. (2) and (3) are generally different.

2.2. Response Matrix Formulation

Eq. (2) is recast into:

$$\mathbf{M}^T \phi = \mathbf{M}^T \mathbf{A}^{-1} s - \mathbf{M}^T \mathbf{A}^{-1} \mathbf{M} J, \tag{4}$$

where $\mathbf{M} \equiv \left[\mathbf{M}_1, \mathbf{M}_2, \cdots\right]$ and $J^T \equiv \left[J_1^T, J_2^T, \cdots\right]$. The element index is dropped for simplicity. Eq. (4) indicates the interface flux moment related to the element source and the surface current moment. Then, the partial current-like variables analogous to the P_1 approximation are defined on the surfaces as:

$$J^{\pm} \equiv \frac{1}{4}\mathbf{M}^T \phi \pm \frac{1}{2} J \,. \tag{5}$$

It should be noted that the weak continuity constraint Eq. (3) is implicitly imposed in Eq. (5). Inserting Eq. (4) into (5) and some mathematical manipulations results in the response matrix (RM) equation as follows:

$$\begin{aligned} J^{+} = &\left(\frac{1}{2}\mathbf{M}^T\mathbf{A}^{-1}\mathbf{M} + \mathbf{I}\right)^{-1}\frac{1}{2}\mathbf{M}^T\mathbf{A}^{-1}s \\ &+\left(\frac{1}{2}\mathbf{M}^T\mathbf{A}^{-1}\mathbf{M} + \mathbf{I}\right)^{-1}\left(\frac{1}{2}\mathbf{M}^T\mathbf{A}^{-1}\mathbf{M} - \mathbf{I}\right)J^{-} \end{aligned} \,. \tag{6}$$

The RM equation is directly used in the solution process with the red-black algorithm or the more general four-color Gauss-Seidel method.

2.3. Equivalence Factors

The converged MOC solution does not satisfy Eq. (1) in general. Therefore, artificial factors should be introduced to make VNM consistent with MOC. A paper dealing with the diffusion acceleration method for a high-order S_N transport solver states that an appropriate projection scheme and nonlinear closure terms ensure consistency [10]. However, it should be noted that MOC cannot generate consistent XS and diffusion coefficients corresponding to higher-order bases. This is because MOC is technically FEM only with the constant basis function, and thus MOC solution space does not include the VNM one. Therefore, only the zeroth moment of flux and current in VNM is ensured to be consistent with the MOC solution.

These zeroth moments are projected from the transport solution as follows:

$$\bar{\phi}_K \equiv \frac{\sum_{k\in K}\phi_k^h V_k}{V_K} \,, \tag{7}$$

$$\bar{J}_E^{\pm} \equiv \frac{\sum_{e\in E} J_e^{h\pm} A_e}{A_E} \,, \tag{8}$$

$$\bar{s}_K \equiv \frac{\sum_{k\in K} s_k^h V_k}{V_K} \,. \tag{9}$$

where k is the fine mesh element index, and e is the fine mesh face index. It should be noted that the MOC mesh involves the coarse mesh on which VNM operates. The superscript h indicates the variable is the high-order solution, and the upper bar means the moment corresponding to the constant basis.

One of the rows in Eq. (2) is the zeroth-moment nodal balance, which is naturally satisfied by the MOC solution. However, higher-order nodal balance is not ensured by the MOC solution generally. Therefore, a residual vector is defined in the element K as follows:

$$v_K \equiv \mathbf{A}_K \phi_K^h + \sum_{E\in K}\mathbf{M}_E\left(J_E^{h+} - J_E^{h-}\right) - s_K^h \,, \tag{10}$$

where the used vectors are given by:

$$\begin{aligned} \phi_K^h &\equiv \left[\bar{\phi}_K, 0, \cdots, 0\right]^T \,, \\ J_E^{h\pm} &\equiv \left[\bar{J}_E^{\pm}\sqrt{A_E}, 0, \cdots, 0\right]^T \,, \\ s_K^h &\equiv \left[\bar{s}_K V_K, 0, \cdots, 0\right]^T \,. \end{aligned}$$

Furthermore, the converged transport solution cannot satisfy the weak continuity because Eq. (3) is established regardless of the MOC formulation. The discontinuity occurs between the interface flux obtained concerning downwind and upwind elements as follows:

$$f_E \equiv \mathbf{M}_{E+}^T \phi_+^h - \mathbf{M}_{E-}^T \phi_-^h \,. \tag{11}$$

This discontinuity can be split into both sides regarding the concerning elements as follows:

$$\mathbf{M}_{E+}^T \phi_+^h + f_{E+} = \mathbf{M}_{E-}^T \phi_-^h + f_{E-} \tag{12}$$

where the residual vectors for downwind and upwind are given by:

$$f_{E+} \equiv -\frac{1}{2} f_E \tag{13}$$

$$f_{E-} \equiv \frac{1}{2} f_E \tag{14}$$

The consistent VNM formulation can be established by using both the residual vectors:

$$\begin{bmatrix} \mathbf{A} & \mathbf{M} \\ \mathbf{M}^T & 0 \end{bmatrix}\begin{bmatrix} \phi \\ J \end{bmatrix} = \begin{bmatrix} s \\ 0 \end{bmatrix} + \begin{bmatrix} v \\ f \end{bmatrix} \,, \tag{15}$$

where $v \equiv \left[v_1, v_2 \cdots\right]^T$ and $f \equiv \left[f_1, f_2, \cdots\right]^T$.

2.4. Consistent Response Matrix Equation

The nodal balance equation is derived from the upper part of Eq. (15) as:

$$\mathbf{A}_K \phi_K + \sum_{E \in K} \mathbf{M}_E J_E = \tilde{s}_K \equiv s_K + v_K \,. \tag{16}$$

Likewise, Eq. (16) is recast into:

$$\mathbf{M}^T \phi \equiv \mathbf{M}^T \mathbf{A}^{-1} \tilde{s} - \mathbf{M}^T \mathbf{A}^{-1} \mathbf{M} J \tag{17}$$

The partial current moment is also constructed with Eq. (12) as:

$$J^{\pm} \equiv \frac{1}{4}\left(\mathbf{M}^T \phi + f\right) \pm \frac{1}{2} J \tag{18}$$

where the residual vector for each surface is chosen by using Eq. (13) or (14) depending on the direction of the surface concerning the element. Eventually, the modified RM equation is established by inserting Eq. (17) into (18) as follows:

$$\begin{aligned} J^{+} = &\left(\frac{1}{2}\mathbf{M}^T \mathbf{A}^{-1} \mathbf{M} + \mathbf{I}\right)^{-1} \frac{1}{2}\left(\mathbf{M}^T \mathbf{A}^{-1} \tilde{s} + f\right) \\ &+ \left(\frac{1}{2}\mathbf{M}^T \mathbf{A}^{-1} \mathbf{M} + \mathbf{I}\right)^{-1} \left(\frac{1}{2}\mathbf{M}^T \mathbf{A}^{-1} \mathbf{M} - \mathbf{I}\right) J^{-} \end{aligned} \tag{19}$$

Note that the volumetric residual vector corrects the volumetric source, while the surface residual vector works as a surface source correction factor. This modified RM equation is a consistent linearized diffusion form with those two correction terms.

2.5. Projection and Prolongation

XS and group constants used in the VNM calculation should be homogenized from the MOC solution. The homogenized quantities are obtained by:

Removal XS: $\Sigma_{rg}^K \equiv \dfrac{\sum_{k \in K} \left(\Sigma_{tg}^k - \Sigma_{sg \to g}^k\right) \phi_{kg}^h V_k}{\sum_{k \in K} \phi_{kg}^h V_k}$,

Scattering XS: $\Sigma_{sg' \to g}^K \equiv \dfrac{\sum_{k \in K} \Sigma_{sg' \to g}^k \phi_{kg'}^h V_k}{\sum_{k \in K} \phi_{kg'}^h V_k}$,

Fission production XS: $\nu\Sigma_{fg}^K \equiv \dfrac{\sum_{k \in K} \nu\Sigma_{fg}^k \phi_{kg}^h V_k}{\sum_{k \in K} \phi_{kg}^h V_k}$,

Fission spectrum: $\chi_g^K \equiv \dfrac{\sum_{k \in K} \chi_g^k \sum_{g'} \nu\Sigma_{fg'}^k \phi_{kg'}^h V_k}{\sum_{k \in K} \sum_{g'} \nu\Sigma_{fg'}^k \phi_{kg'}^h V_k}$,

Diffusion coefficient: $D_g^K \equiv \dfrac{\sum_{k \in K} \frac{1}{3\Sigma_{tg}^k} \phi_{kg}^h V_k}{\sum_{k \in K} \phi_{kg}^h V_k}$.

Zeroth moments of flux and partial current are projected using Eq. (7) and (8). The flux moment is directly set to the initial value of a VNM calculation. However, the initial partial current moments are not set to Eq. (8) because partial currents obtained by a transport calculation do not have to do with the diffusion theory. This value is set as Eq. (18), where only the net current moment is projected from the MOC calculation.

There are two options for prolongation operators: multiplicative and additive ones. These do not affect the solution but convergence behavior. It is shown that the additive prolongation requires one more MOC outer iteration in general. Therefore, the multiplicative prolongation is set as default for now.

2.6. Solution Procedure

Overall solution sequence follows the ordinary VNM solution algorithm but involves the XS homogenization and the projection of flux and current before the red-black iteration. The equivalence factors are obtained with the projected moments as Eq. (10) and (12). Then, the red-black algorithm solves the RM equation constructed with these homogenized quantities, as summarized in Algorithm 1.

Algorithm 1. Consistent VNM solution procedure.

```
Project zeroth flux and partial current moments
Homogenize XS and group constants
Generate volumetric and surface equivalence factors
for fission source iteration do
    Calculate fission source
    for scattering source iteration do
        Update volumetric source with Eq. (10)
        Update surface source with Eq. (12)
        for fixed source iteration do
            Solve Eq. (19) with the red-black algorithm
        end for
    end for
    Update fission source and eigenvalue
    if converged enough break
end for
```

3. Verification and Examination

The method is implemented in the NuDEAL code. The VNM polynomial orders are set to 2 and 0 for flux and current approximations, respectively. Although the higher-order moments do not affect solution accuracy, the full-rank condition forces the nodal balance system to have a minimum rank for stable convergence [11]. The C5G7 [12] 2D problems are adopted for investigations.

3.1. Effects of Equivalence Factors

The UO_2 assembly is chosen as the test problem. Its mesh configurations are depicted in Figure 1. The pin-wise regular grid is used in the VNM calculation. The MOC calculation is performed so that the fission source

and eigenvalue errors converge to 10^{-10}. Then, the VNM calculation is performed with the converged solution. To examine the effects of the two equivalence factors, VNM calculations without the factors are also performed. The results are illustrated in Table I, demonstrating that the eigenvalue errors occur when one of the factors is not applied.

This inconsistency is also revealed in the fission source convergence behavior when MOC and VNM are performed alternately, as illustrated in Figure 2. The fission source does not converge when any correction factor is not applied. Therefore, it is confirmed that both correction factors are essential to generating a VNM solution consistent with MOC.

3.2. Irregular Grid Compatibility

NuDEAL features a low-order calculation using an irregular coarse mesh generated by a stencil grid input. Figure 3 illustrates irregular grids used in the assembly test problem. The convergence behavior is investigated for such partitioned coarse mesh. Figure 4 shows the results, confirming that the MOC/VNM scheme converges well, regardless of the grid regularity.

3.3. Acceleration Effectiveness Comparison

The C5G7 2D core and its mockup configuration are solved. The core size is expanded by adding two rows of fuel assemblies, both in horizontal and vertical directions. Pin-wise regular coarse meshes are used. VNM and CMFD are compared from the perspective of acceleration efficiency. Figure 5 shows that CMFD acceleration requires 7 MOC outer iterations, while VNM needs 8. VNM is also effective as a low-order acceleration method.

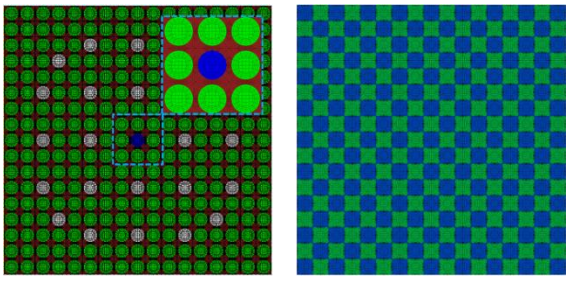

Figure 1. Fine and coarse meshes of test problem.

Table I. Eigenvalues of MOC and VNM calculations.

	(V.C.[a]/S.C.[b])	Eigenvalue (Diff.)
MOC/VNM	None	1.335407 (180 pcm)
	V.C.	1.337157 (354 pcm)
	S.C.	1.331857 (-175 pcm)
	Both	1.333611
MOC (Ref.)		1.333611

[a] volumetric correction factor
[b] surface correction factor

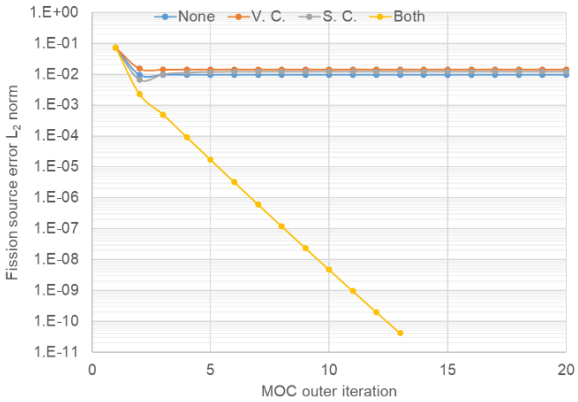

Figure 2. Fission source convergence according to correction factor.

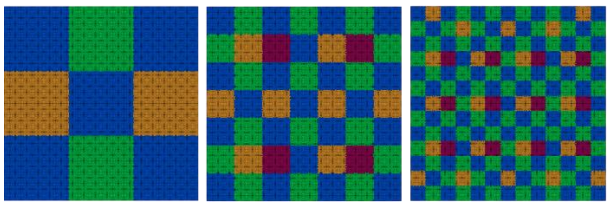

Figure 3. Stencil grid examples: 3×3, 7×7, and 13×13.

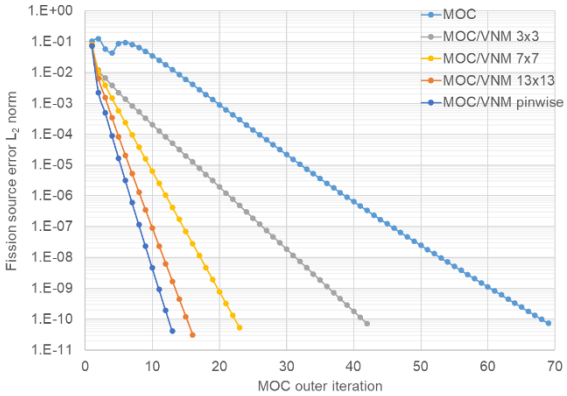

Figure 4. Convergence behavior of MOC/VNM depending on the mesh regularity.

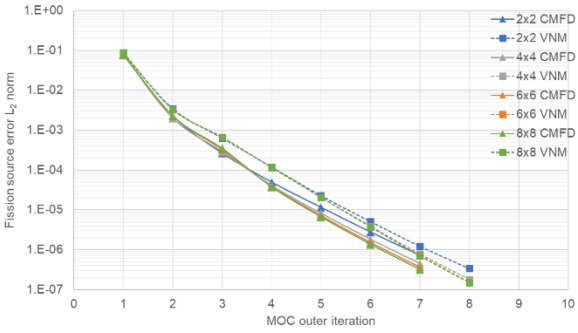

Figure 5. Acceleration effects of CMFD and VNM.

4. Conclusion

The low-order diffusion VNM is formulated so that the VNM calculation is consistent with the high-order MOC calculation. Contrary to the nonlinear diffusion acceleration for higher-order FEM calculations [10], MOC cannot provide consistent physical coefficients corresponding to the higher-order bases. Therefore, artificial correction factors are introduced for the nodal balance equation and the surface flux weak continuity, respectively. These equivalence factors work as correction terms to the volumetric and surface sources, forming a weak linearized diffusion form. The effects of those equivalence factors are examined, and it is confirmed that they should be simultaneously applied to produce MOC-consistent VNM solutions. Furthermore, this scheme is compared with CMFD for the low-order acceleration method. It is shown that the consistent VNM works as the acceleration method well, and only one more outer iteration is needed than CMFD.

The NuDEAL solution capability will be extended to 3D problems with the developed MOC/VNM solution scheme. As planar MOC is embedded in 3D orthogonal S_N [13], this developed scheme forms a 2D/3D method where planar MOC solves a fine mesh 2D domain, and the consistent VNM solves the entire 3D domain. The acceleration effects of VNM will be investigated even under the 3D problems. If the diffusion VNM cannot produce sufficiently accurate solutions due to strong axial heterogeneity, VNM based on P_N or SP_N (simplified P_N) should be employed. It is anticipated that a similar equivalence can be formulated for P_N or SP_N VNM.

ACKNOWLEDGEMENTS

This work was supported by the National Research Foundation of Korea (NRF) grant funded by the Korea government (MSIT) (No. 2021M2D6A1048220).

REFERENCES

[1] C. Lee *et al.*, “Griffin Software Development Plan,” ANL/NSE-21/23, INL/EXT-21-63185, 2021.

[2] A. Marin-Lafleche, M. A. Smith, and C. Lee, “Proteus-MOC: A 3D deterministic solver incorporating 2D method of characteristics,” in *International Conference on Mathematics and Computational Methods Applied to Nuclear Science and Engineering*, 2013, pp. 2759–2770.

[3] K. M. Kim, H. G. Lee, and H. G. Joo, “GPU-based Method of Characteristics with CMFD Acceleration in Unstructured Mesh Geometry Transactions of the Korean Nuclear Society Sprint Meeting,” in *Transactions of the Korean Nuclear Society Spring Meeting*, 2023.

[4] K. M. Kim, H. G. Lee, J. Yoon, and H. G. Joo, “GPU-accelerated Method of Characteristics with Discontinuous Galerkin Method in Unstructured Mesh Geometry,” in *International Conference on Mathematics and Computational Methods Applied to Nuclear Science and Engineering*, 2023.

[5] I. Dilber and E. E. Lewis, “Variational Nodal Methods for Neutron Transport,” *Nucl. Sci. Eng.*, vol. 91, no. 2, pp. 132–142, Oct. 1985, doi: 10.13182/NSE85-A27436.

[6] P. A. Raviart and J. M. Thomas, “Primal hybrid finite element methods for 2nd order elliptic equations,” *Math. Comput.*, vol. 31, no. 138, pp. 391–413, 1977, doi: 10.1090/s0025-5718-1977-0431752-8.

[7] G. Palmiotti, E. E. Lewis, and C. B. Carrico, “VARIANT: VARIational Anisotropic Nodal Transport for Multidimensional Cartesian and Hexagonal Geometry Calculation,” Argonne National Laboratory, ANL-95/40, 1995.

[8] J. Y. Doriath *et al.*, “Reactor analysis using a variational nodal method implemented in the ERANOS system,” in *Topical Meeting on Advances in Reactor Physics*, 1994, pp. 11–15.

[9] T. Zhang and Z. Li, “Variational nodal methods for neutron transport: 40 years in review,” *Nucl. Eng. Technol.*, vol. 54, no. 9, pp. 3181–3204, 2022, doi: 10.1016/j.net.2022.04.012.

[10] S. Schunert *et al.*, “A flexible nonlinear diffusion acceleration method for the SN transport equations discretized with discontinuous finite elements,” *J. Comput. Phys.*, vol. 338, pp. 107–136, Jun. 2017, doi: 10.1016/j.jcp.2017.01.070.

[11] C. B. Carrico, E. E. Lewis, and G. Palmiotti, “Matrix Rank in Variational Nodal Approximations,” in *Transactions of the American Nuclear Society*, 1994, p. 162.

[12] OECD NEA, “Benchmark on deterministic time-dependent transport calculations without spatial homogenisation,” Nuclear Energy Agency Organisation for Economic Cooperation and Development, NEA/NSC/DOC(2003)16, 2003.

[13] M. T. H. Young, B. Collins, and W. R. Martin, “2-D/3-D Reactor Analysis using Orthogonal-Mesh SN with Embedded 2-D Method of Characteristics,” in *International Conference on Mathematics and Computational Methods Applied to Nuclear Science and Engineering*, 2017.